Two-Parameter Study of the Quasiperiodic Route to Chaos in Convecting ^{3}He–Superfluid-^{4}He Mixtures

Ronnie Mainieri
New York University, 14 Washington Place, New York, New York 10003

Timothy S. Sullivan and R. E. Ecke
Physics Division and Center for Nonlinear Studies, Los Alamos National Laboratory, Los Alamos, New Mexico 87545
(Received 12 December 1988)

We study the frequency lockings of two intrinsic hydrodynamic modes of a convecting ^{3}He–superfluid-^{4}He mixture by independently varying the Rayleigh and Prandtl numbers. We establish points on the critical line in this parameter space using a transient technique to locate the spiral-node transition in the interior of three resonance horns. Universal scaling is demonstrated at winding numbers with golden-mean tails by computing the $f(\alpha)$ singularity spectrum.

PACS numbers: 47.25.−c, 05.45.+b, 67.60.Fp

The transition to chaos involving two incommensurate frequencies has attracted great theoretical and experimental interest. Theoretical predictions of global and local universality are based on one-dimensional circle-map models such as the sine circle map[1–7] and include scaling indices,[1–3] $f(\alpha)$ singularity spectra,[4,5] and trajectory scaling functions.[6,7] Experimental verification of this route to chaos has been made only for systems with an internal periodic oscillation modulated by an external drive of variable frequency and amplitude.[8–10] In the more general case of two internal frequencies which exhibit quasiperiodicity and mode locking,[11,12] no comparison has been made owing to the difficulty of varying two internal control parameters over an appropriate region of parameter space. Natural quasiperiodic states are fundamentally different than driven ones because the additional degree of freedom of the second internal mode allows for feedback between the two oscillators. If predictions of universality can be experimentally verified for such states it would constitute a major extension of the theory.

In this Letter we report the first measurement of universal scaling properties in natural two-frequency quasiperiodicity. We locate the critical line in the experimental parameter space using a novel transient Poincaré-section technique and demonstrate predicted universality using a thermodynamic singularity-spectrum analysis of experimental data taken at winding numbers with golden-mean tails [the two experimental frequencies do not naturally lock to a ratio close to the golden-mean ratio of $\omega_g \equiv (\sqrt{5}-1)/2$]. We also present a new method to compute $f(\alpha)$ singularity spectra which has superior convergence properties to those of other reported techniques.[4,6]

The experimental system, described in detail elsewhere,[11] is Rayleigh-Bénard convection of a ^{3}He-superfluid-^{4}He mixture at temperatures close to 0.85 K. When heated from above, this system behaves as a classical single-component fluid undergoing thermal convection. In this system Haucke and Ecke[11] discovered a rich and extensive region of quasiperiodicity and mode locking using a local measure of the fluid temperature field as the experimental probe of system dynamics. This region is defined in terms of two dimensionless parameters: the Rayleigh number R, proportional to the temperature difference across the fluid layer, and the Prandtl number σ. In our system, we can vary σ over a substantial range ($0.04 < \sigma < 0.15$) by varying the mean temperature, thereby allowing us enough control over R and σ to perform a two-parameter study of quasiperiodicity and mode locking. At fixed σ the fundamental frequencies of the two internal modes, f_1 and f_2, change rapidly with increasing R, and the winding number (defined as $\rho = f_2/f_1$) sweeps through many mode-locked intervals. As σ is decreased the coupling between modes increases as evidenced by the widening and eventual overlap of resonance horns and by complex internal structure interior to the horn boundaries. In Fig. 1 we show resonance horns in the R-σ parameter space which are bounded at small R by the 1/7 resonance and at large R by the 1/6 resonance. Also shown are lightly shaded regions indicating hysteresis and some of the internal structure of the 2/13 resonance.[13] One can roughly identify R as proportional to Ω (the bare winding number) and $1/\sigma$ as proportional to k, the nonlinearity parameter in the sine circle map defined as

$$\theta_{n+1} = \theta_n + \Omega - (k/2\pi)\sin(2\pi\theta_n) . \quad (1)$$

For $k > 0$ the average rotation per iterate ω is, in general, not equal to Ω and can take on rational values over finite intervals in Ω, i.e., mode-locked intervals with $\omega = P/Q$, P and Q integer. The map loses its invertibility at $k = 1$ and chaos becomes possible at special irrational numbers where universal predictions for the transition from quasiperiodicity to chaos should apply.[1–5]

In the circle map the critical line occurs at $k = 1$, but

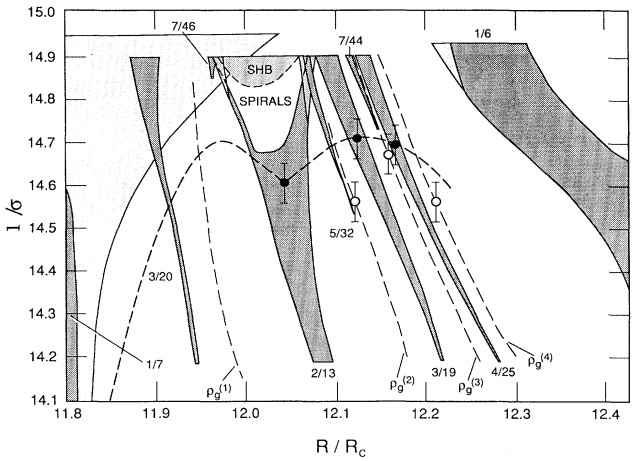

FIG. 1. Resonance horns in parameter space of inverse Prandtl number, $1/\sigma$ vs normalized Rayleigh number R/R_c. Dashed lines indicate golden-mean lines with winding numbers $\rho_g^{(1)}$, $\rho_g^{(2)}$, $\rho_g^{(3)}$, and $\rho_g^{(4)}$. Lightly shaded regions indicate hysteresis; the interior structure of the 2/13 horn consists of regions of stable "spiral" periodic cycles and secondary Hopf bifurcation SHB of those periodic cycles. Also shown are estimated locations of the critical line from analysis of spiral periodic cycles (●) and where $f(a)$ was calculated (○).

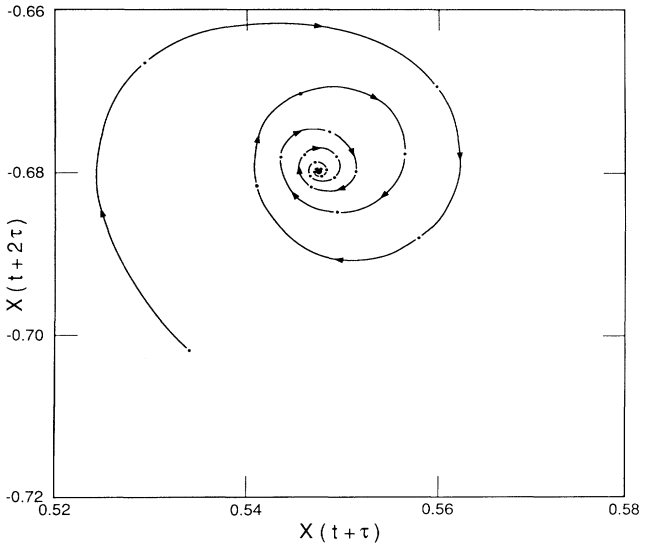

FIG. 2. Transient Poincaré section showing spiral approach to a periodic point in the 2/13 resonance horn; $R/R_c = 12.025$ and $1/\sigma = 14.77$. The solid curves are guides to the eye.

in the experimental parameter space the critical line may be quite complex and irregular. This was suggested by a two-dimensional map simulation[14,15] in which the critical line was defined as the set of points along which the invariant circle loses its smoothness. One place this occurs is in the interior of a resonance horn where the periodic points change from nodal stability (two real eigenvalues) to spiral stability (complex conjugate eigenvalues), destroying the smooth invariant curve. We similarly consider the critical line in the experiment to consist of the locus of the minima of $1/\sigma$ values for which a spiral periodic point exists inside each resonance horn. To locate the spiral fixed points we analyze transient Poincaré sections, produced by a step change in R. At each edge of a horn the eigenvalues of the periodic points are both real since mode locking occurs as a saddle-node bifurcation on the invariant circle. In the interior, however, the eigenvalues can become complex. As an example, in Fig. 2 we show a spiral periodic cycle in the 2/13 resonance horn from which we extract both the radial contraction rate λ_r and the angular rotation rate λ_i. In Fig. 3 we show the radial and angular eigenvalues as functions of R/R_c for $1/\sigma = 14.77$. For $14.56 < 1/\sigma < 14.66$ we can not distinguish between real and complex eigenvalues. For $1/\sigma < 14.56$ there are two real eigenvalues. The difficulty in distinguishing spirals, when the two eigenvalues are nearly equal, sets our resolution of the critical line which we estimate to be at $1/\sigma = 14.62 \pm 0.03$ for $R/R_c = 12.05$. Similar measurements of the 3/19 and 4/25 horns yield spiral transitions at $1/\sigma = 14.72 \pm 0.04$ ($R/R_c = 12.12$) and $1/\sigma = 14.70 \pm 0.04$ ($R/R_c = 12.17$),

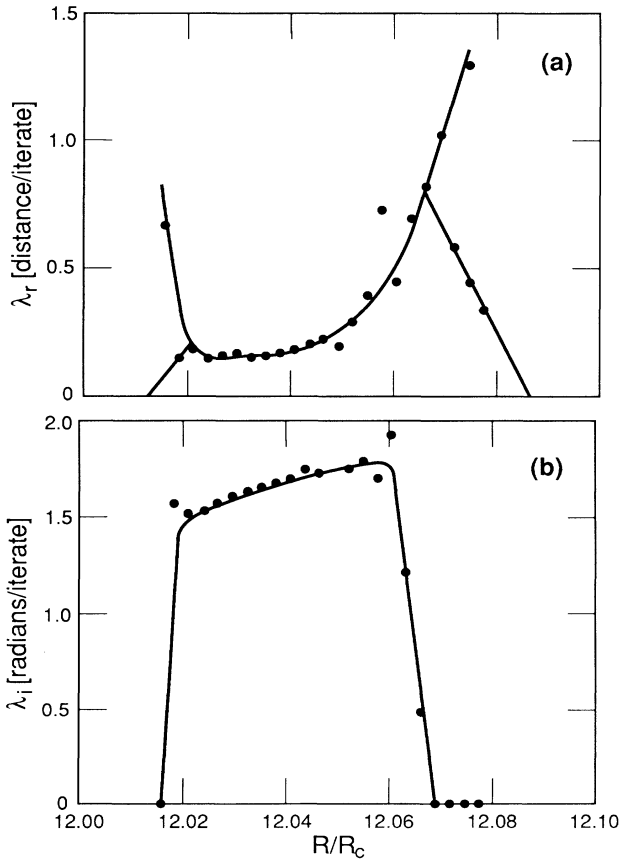

FIG. 3. Eigenvalues for 2/13 resonance horn vs R/R_c with $1/\sigma = 14.77$. (a) Radial contraction rate λ_r in units of phase-space distance per iterate; (b) angular rotation rate λ_i in units of radians per iterate. The solid curves are guides to the eye.

respectively. In Fig. 1 we have drawn the critical line as determined by the spiral-node transitions and by upper bounds imposed by hysteresis regions. The lines labeled $\rho_g^{(n)}$ in Fig. 1 are defined by winding-number sequences $1/[6+1/[n+1/[1+1/[1+\cdots]]]]$. At the crossings of the critical line and any of these lines of constant $\rho_g^{(n)}$ we expect to observe universal behavior. (These winding numbers have the same asymptotic form as the golden mean and thus should have the same universal scaling properties.) In particular we can compare experimentally obtained $f(\alpha)$ curves with theoretical results.

The experimental data consist of time series from the local temperature sensor.[11] From the data we reconstruct the attractor using delay coordinates and obtain Poincaré sections as the intersection of phase-space trajectories with a plane in that space. An example of the Poincaré sections we obtain is shown in Fig. 4 for parameter values $R/R_c=12.220$ and $1/\sigma=14.57$, close to criticality, with a rotation number within 50 ppm of $\rho_g^{(4)}$ [the effective rotation number ω of the section is related to the winding number of ρ by $\omega=1/\rho$ (mod1)]. We can approximate the section by a periodic cycle with winding number P/Q, where P/Q is rational approximant to ρ. For this cycle the closest point in space to some initial point on the section occurs after r time steps, where r satisfies $rP=1$ (mod$Q$). We use this to determine a series of consecutive segments Δ_k along the section. In the inset of Fig. 4 we see the union of these segments for $P/Q=18/129$ and the smooth, linelike nature of the section. If the manifold is not one dimensional, as happens for higher values of $1/\sigma$, then there is no choice of r that gives a smooth curve.

Using these segments we would like to establish that the data in Fig. 4 were generated by a dynamics in the same universality class as the cubic circle map. We will do so by comparing the multifractal properties of the experimental attractor with those given by the renormalization group (RG) calculations. We use a "thermodynamic" formalism[6] and interpret the segments as states of a statistical mechanical system. The "pressure"

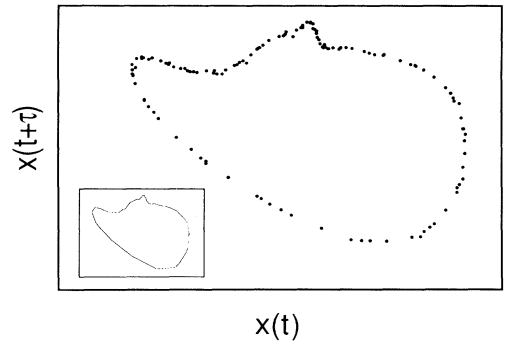

FIG. 4. Poincaré section for $R/R_c=12.220$, $1/\sigma=14.57$, and ρ within 50 ppm of $\rho_g^{(4)}$ and with $\tau=(7f_2)^{-1}$. Inset: Connected segments as discussed in text.

$p(\beta)$ is given by

$$p(\beta)=-\lim_{Q\to\infty}\sum_{1\le k\le Q}|\Delta_k|^{\beta}/\ln Q\,. \tag{2}$$

From the pressure we can compute its derivative, the "energy" $u(\beta)$, and the "entropy" $s(\beta)=\beta u-p$, and use these to implicitly compute the singularity spectrum $f(\alpha)=s/u$, with $\alpha=1/u$. We have directly verified that the limit in (2) exists by plotting the right-hand side as a function of Q and seeing that it converges as $(\ln Q)^{-1}$. For monotonic circle maps at golden-mean tail rotation number the theoretical pressure can be approximated to within 1% by two parameters,[6] s_1 and s_2, with $p(\beta)=-\ln z(\beta)/\ln\omega_g$ and z being the smallest root of

$$z^3(1-s_1)^{\beta}(1-s_2)^{\beta}-(1-s_1^{\beta}z)(1-s_2^{\beta}z^2)=0\,. \tag{3}$$

The two parameters exactly give the range of α ($\alpha_{\min}=\ln\omega_g/\ln s_1$ and $\alpha_{\max}=2\ln\omega_g/\ln s_2$) and can be computed from the RG universal function. If we compute $f(\alpha)$ directly from (2) or by the Legendre transform of the generalized dimensions,[4] we are effectively determining s_1 and s_2 from just two segments: the smallest and the largest among the Q segments. In the cubic circle map the largest segment converges with a factor $(1.288\,57\ldots)^{-\ln Q}$, and thus very long cycles are required for an accurate determination of $f(\alpha)$. Our method then is to compute the pressure from the definition (2), obtain z, and then use a nonlinear least-squares fit to determine the two universal scales s_1 and s_2 in (3). To avoid using just two of the segments we include only pressure values for small $|\beta|$, i.e., the transition region of the energy. More details will be given elsewhere.[16] We have verified that the method is insensitive to the precise cutoff in β. Along the line $\rho_g^{(4)}$ we obtain

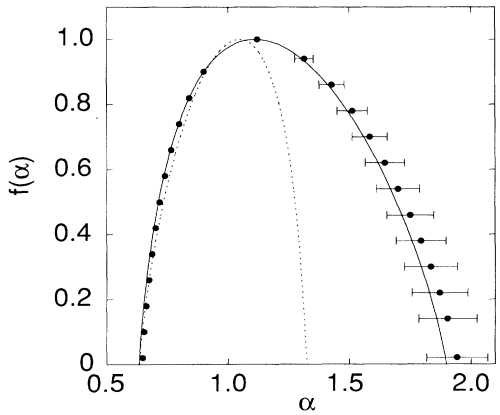

FIG. 5. The $f(\alpha)$ curve obtained from the experimental data of Fig. 4 (●). The solid curve is the $f(\alpha)$ curve for a map in the sine-circle-map universality class. The error bars for α smaller than 1.1 are of the order of the circles and are not plotted. The dashed line is computed from a subcritical data set with $R/R_c=12.375$ and $1/\sigma=14.17$.

$s_1 = 0.47 \pm 0.01$ and $s_2 = 0.61 \pm 0.2$. The values predicted by the RG calculations for a cubic map are $s_1 = 0.467$ and $s_2 = 0.602$. Using fitted values we obtain the $f(\alpha)$ curve in Fig. 5. The scatter of s_1 and s_2 give us a range for the $f(\alpha)$ spectra and we use this to determine the error bars on the plot. Also, in the figure we have plotted $f(\alpha)$ for a subcritical data set.

From s_1 and s_2 we can compute the value of the exponent that characterizes the universality class of a map. If we consider inflection points of the type $\theta | 2\theta |^{\nu-1}$, then we can compute that $\nu = 2 \ln s_1 / \ln s_2$. From the data for the rotation number $\rho_g^{(4)}$ we get that $\nu^{(4)} = 3.1 \pm 0.3$, putting the data in the universality class of the sine circle map [Eq. (1)]. The other rotation numbers give similar results, $\nu^{(2)} = 2.9 \pm 0.3$ and $\nu^{(3)} = 2.8 \pm 0.4$, whereas the series for $\rho^{(1)}$ fails to exhibit criticality.

We acknowledge conversations with I. G. Kevrekidis. One of us R.M. would like to thank the Center for Nonlinear Studies for its hospitality and support and to acknowledge suggestions by J. Lowenstein. This work was supported by funds provided by the Department of Energy, Office of Basic Energy Sciences, Division of Material Science.

[1]S. Shenker, Physica (Amsterdam) **5D**, 405 (1982); M. Feigenbaum, L. P. Kadanoff, and S. Shenker, Physica (Amsterdam) **5D**, 370 (1982); S. Ostlund, D. Rand, J. Sethna, and E. Siggia, Phys. Rev. Lett. **49**, 132 (1982); Physica (Amsterdam) **8D**, 303 (1983).

[2]M. Jensen, P. Bak, and T. Bohr, Phys. Rev. A **30**, 1960 (1984).

[3]P. Cvitanović, M. Jensen, L. Kadanoff, and I. Procaccia, Phys. Rev. Lett. **55**, 343 (1985).

[4]H. Hentschel and I. Procaccia, Physica (Amsterdam) **8D**, 435 (1983); T. Halsey, M. Jensen, L. Kadanoff, I. Procaccia, and B. Shraiman, Phys. Rev. A **33**, 1141 (1986).

[5]M. Jensen, L. Kadanoff, A. Libchaber, I. Procaccia, and J. Stavans, Phys. Rev. Lett. **55**, 2798 (1985).

[6]M. Feigenbaum, J. Stat. Phys. **46**, 919 (1987); **46**, 925 (1987).

[7]M. J. Feigenbaum, Nonlinearity **1**, 577 (1988); Commun. Math. Phys. **77**, 65 (1980).

[8]J. Stavans, F. Heslot, and A. Libchaber, Phys. Rev. Lett. **55**, 596 (1985).

[9]D. Olinger and K. Sreenivasan, Phys. Rev. Lett. **60**, 797 (1988).

[10]E. Gwinn and R. Westervelt, Phys. Rev. Lett. **59**, 156 (1987).

[11]H. Haucke and R. Ecke, Physica (Amsterdam) **25D**, 307 (1987).

[12]A. Libchaber, S. Fauve, and C. Laroche, Physica (Amsterdam) **7D**, 73 (1983); J. Gollub and S. Benson, J. Fluid Mech. **100**, 449 (1980); M. Dubois and P. Berge, Phys. Lett. **76A**, 53 (1980).

[13]R. Ecke and I. Kevrekidis, Phys. Lett. A **131**, 344 (1988).

[14]T. Bohr, Phys. Rev. Lett. **54**, 1737 (1985).

[15]X. Wang, R. Mainieri, and J. Lowenstein (to be published).

[16]R. E. Ecke, R. Mainieri, and T. S. Sullivan (to be published).

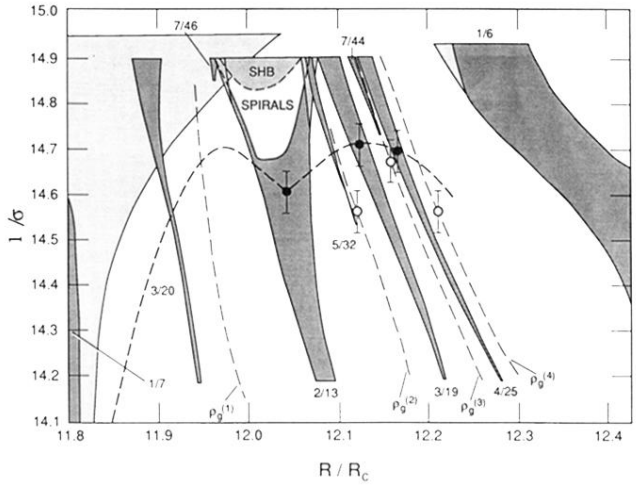

FIG. 1. Resonance horns in parameter space of inverse Prandtl number, $1/\sigma$ vs normalized Rayleigh number R/R_c. Dashed lines indicate golden-mean lines with winding numbers $\rho_g^{(1)}$, $\rho_g^{(2)}$, $\rho_g^{(3)}$, and $\rho_g^{(4)}$. Lightly shaded regions indicate hysteresis; the interior structure of the 2/13 horn consists of regions of stable "spiral" periodic cycles and secondary Hopf bifurcation SHB of those periodic cycles. Also shown are estimated locations of the critical line from analysis of spiral periodic cycles (●) and where $f(\alpha)$ was calculated (○).